IEEE Access
Multidisciplinary | Rapid Review | Open Access Journal

Received 1 July 2024, accepted 15 July 2024, date of publication 17 July 2024, date of current version 26 July 2024.

Digital Object Identifier 10.1109/ACCESS.2024.3429552

RESEARCH ARTICLE

Design Optimization and Comparative Study of Skewed Halbach-Array Magnets TORUS Axial-Flux Permanent Magnet Motors for Electric Vehicles

PHUSON SRIKHUMPHUN[1], PATTASAD SEANGWONG[1], JONGGRIST JONGUDOMKARN[1], APIRAT SIRITARATIWAT[1], NUWANTHA FERNANDO[2], SAKDA SOMKUN[3], (Senior Member, IEEE), AND PIRAT KHUNKITTI[1], (Senior Member, IEEE)

[1]Department of Electrical Engineering, Faculty of Engineering, Khon Kaen University, Khon Kaen 40002, Thailand
[2]School of Engineering, Royal Melbourne Institute of Technology (RMIT), Melbourne, VIC 3000, Australia
[3]School of Renewable Energy and Smart Grid Technology (SGtech), Naresuan University, Phitsanulok 65000, Thailand

Corresponding author: Pirat Khunkitti (piratkh@kku.ac.th)

This work was supported in part by the National Research Council of Thailand and Khon Kaen University under Grant N42A660360; and in part by the Research Fund of the Faculty of Engineering, Khon Kaen University, through the Research Scholarship for M.Eng. Students Project under Contract M-EE-2023/003.

ABSTRACT The double-sided axial flux (TORUS) permanent magnet (PM) machine has been shown to be an efficient structure for electric vehicles (EVs). This paper introduces the combined techniques of skewed PMs and Halbach-array arrangement to improve the TORUS-type axial flux PM motor performance. The suitable configuration for implementing this combination in the TORUS PM machine was investigated, considering two possible models. Each model of the skewed Halbach-array PM TORUS motor is optimized using response surface methodology to meet the performance requirements of an EV application. A comparative evaluation of machine performance via 3D finite element analysis is performed and detailed insight into the design and configuration of the skewed Halbach-array PM TORUS machine is presented. Under no-load conditions, the optimal skewed Halbach-array PM TORUS motor exhibits 4% higher back-EMF and 9.3% lower cogging torque compared to a benchmark TORUS motor. During on-load operation, the proposed motor shows an 8% increase in average torque compared to the benchmark, accompanied by a significant 7.8% reduction in torque ripple. The rationale behind this enhanced torque capability is explained in detail and is found to be due to enhanced flux-concentration and flux-cancellation effects within the motor. The efficiency of the proposed TORUS motor is enhanced. The results confirm the superiority of the combined skewed Halbach PM Array techniques to improve TORUS PM motor performance and suggest suitable configurations for this combined technique in EV motors.

INDEX TERMS Axial flux permanent magnet machines, double-sided axial flux machines, skewed permanent magnet, Halbach permanent magnet arrangement, electric vehicles.

I. INTRODUCTION

The advent of electric vehicles (EVs) signifies a significant shift in transportation, providing environmentally friendly mobility options while addressing issues associated with traditional internal combustion engines [1], [2], [3], [4]. Permanent magnet (PM) machines have become widely utilized as electric motors in EVs, capitalizing on their notable benefits such as superior efficiency, torque density, and the elimination of field excitation [5], [6], [7], [8]. Axial flux permanent magnet (AFPM) motors have emerged as an attractive choice for EV propulsion due to their

The associate editor coordinating the review of this manuscript and approving it for publication was Emanuele Crisostomi.

impressive power density and cost-effective production methods [9], [10], [11]. Particularly, axial flux double-sided motors referred to as the TORUS motor, characterized by a single stator core positioned between two rotors, have garnered attention in recent EV studies for their outstanding attributes [12]. These motors demonstrate high torque density per PM volume, enhanced efficiency, and a wide operating speed range. Moreover, they offer the advantage of streamlining the manufacturing process by reducing the number of components in the motor compared to other AFPM motors [12], [13].

Previous developments in TORUS and other type of AFPM motors for EVs have concentrated on improving torque density, reducing torque ripple and cogging torque, and enhancing efficiency [5], [14], [15]. Nonetheless, a significant challenge continually being investigated is the possibility to either maintain or decrease magnet volume while increasing torque per unit volume. To achieve this objective, various methods have been investigated, including adjusting pole combinations, modifying stator shoes, altering PM shapes, changing iron core materials, employing Halbach-array PM configurations, and employing skewed magnet techniques. Particularly, an intriguing approach to enhancing machine performance involves adjusting the PM configuration such as shaping, Halbach-array arrangements, and skewed magnet techniques. These methods appear readily achievable without incurring extra costs and while ensuring the possibility to maintain or reduce the total PM volume. The fundamental idea behind these techniques is to optimize magnetic field utilization and concentrate flux within the structure to enhance machine performance. Numerous literature surveys have performed several of the above-mentioned techniques to improve the performance of AFPM motors.

In 2006, the skewing PM technique was considered by the authors on [9] to minimize torque ripple in AFPM motors. The research highlighted the significant enhancement in torque capability of TORUS configuration among various AFPM designs. In 2021, an optimized stator shaping technique was applied for single-sided AFPM motors by segmenting and adjusting stator segments, resulting in decreased cogging torque and improved machine efficiency [10]. Another investigation using an N-N configuration where a north pole faces another north pole in TORUS motors with skewed PMs [16] demonstrated a notable reduction in torque ripple and simultaneously enhancing the machine's torque capability. Similarly, a method employing skewed PMs, derived from the configuration of a single skewed PM technique was developed to reduce cogging torque in yokeless and segmented armature (YASA) AFPM motors [16]. This technique involved the adjustment of multiple magnet angles, demonstrating a significant reduction of the YASA machine cogging torque. Additionally, Z. Islam et al. conducted a comparative study of various geometric shapes of TORUS-type motors to identify the most efficient structure [17]. Among these shapes, the arc-shaped rotor configuration demonstrated the highest efficiency and torque performance. Furthermore, a technique proposing an angled triangular right pentagon shape was introduced to enhance torque per magnet volume and reduce torque ripple of AFPM motors in [18].

In 2016, the concept of transforming from a conventional PM configuration to a Halbach-array PM arrangement for TORUS motors was introduced [19]. This arrangement substantially increased torque per unit volume due to improved magnetic field utilization. Subsequent studies have also utilized Halbach-array PM arrangements to enhance the performance of AFPM motors. In 2019, Z. Zhang et al. aimed to enhance AFPM machine performance at high rotational speeds by optimizing the design of the Halbach-array PMs in the rotor [20], resulting in significantly improved performance in the high-speed range. In another advancement in 2021, a novel AFPM structure combining radial and axial flux with Halbach-array PMs was proposed to intensify magnetic flux density in the air gap [21]. This research identified a correlation between PM magnetization orientation and the number of segments per pole pair. The recent tendency of employing Halbach-array PM arrangements persists in current research. For example, C. Huang et al. [22] employed the Halbach-array technique at the outer rotor and stator core, optimizing machine design parameters and demonstrating enhanced machine performance.

Past research demonstrates the substantial performance enhancement that can be achieved by employing the skewed magnet technique or the Halbach PM arrangement in AFPM machines. While each of these two techniques has been independently utilized, their combination has not yet been explored and implemented in AFPM machines. Therefore, this research aims to address this gap in the current literature by introducing a combined approach of skewed magnet and Halbach-array PM techniques with application to a TORUS motor design. Since this combination is being introduced for the first time, it is crucial to investigate the appropriate approach for applying this combination in the TORUS motor, an aspect that has not been previously discussed or evaluated. These unexplored aspects offer significant potential for gaining insights into the advantages and trade-offs associated with these specific configurations. In this context, the contributions of this work are: 1) Introduction of the combined application of skewed magnet and Halbach-arrays PM techniques in an AFPM TORUS machine and 2) The comparative analysis and design optimization of the configuration of the skewed magnet and Halbach-arrays PM rotor of the TORUS motor using 3D finite element analysis simulations.

Section II of this paper explains the topology of the skewed Halbach-array PM TORUS motor. Section III details the design procedure encompassing the selection of design variables, and optimization process using response surface methodology (RSM). Section IV evaluates the performance of the candidate machine and compares it with a benchmark machine. Finally, Section V presents the conclusions of this research.

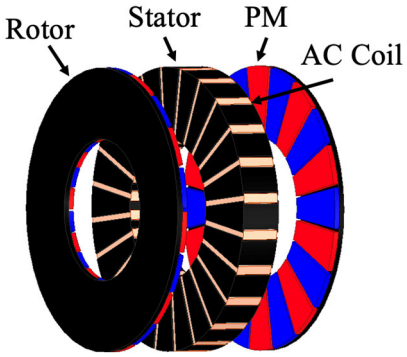

FIGURE 1. Topology of the benchmark TORUS PM motor.

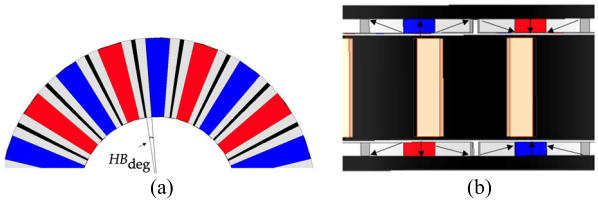

FIGURE 2. Configuration of dual skewed PMs in the proposed.

II. MACHINE TOPOLOGIES

In this study, we adopt a state-of-the-art TORUS PM motor previously developed in [23] as a baseline for comparison. As shown in Fig. 1, the benchmark three-phase TORUS motor contains 24-stator slots/20-rotor poles. It is assembled by a single stator core positioned between two rotors. The structure employs a concentrated winding. Each rotor pole contains NdFeB PM with adjacent pole having opposite polarity. Soft magnetic composite (SMC) material is used for the core to achieve low core losses, enhance magnetic permeability, and improved efficiency. This TORUS PM motor is selected for benchmarking purposes in this study due to its high torque density which ranks very high compared to the other AFPM motors existed in the literature, as well as its features well suited for EV applications. The rotor of the proposed skewed Halbach-arrays PM TORUS motor is designed by arranging the PMs into a Halbach-array which features the center magnet sandwiched between two adjacent magnets. The center magnet in a Halbach array typically functions as the primary magnet, indicating the main direction of magnetic flux circulation. Additionally, it has a substantially larger volume compared to the two adjacent magnets, which consequently serve as secondary magnets.

As shown in Fig. 2, the magnetization of secondary magnets is set as 45 degrees with respect to the magnetization orientation of the primary magnet in order to enhance the concentration of air-gap magnetic flux and the magnetic flux circulation within the rotor. The magnetization of the sandwiching magnets pointing to the stator is set to be 45 degrees pointing into the center magnet magnetization orientation, while that of the sandwiching magnets pointing to the rotors is set to be 45 degrees out of the center

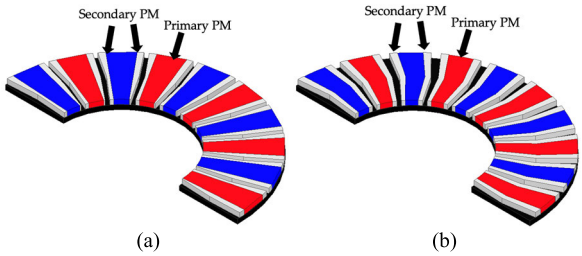

FIGURE 3. Configuration of the proposed skewed Halbach-array PMs rotors. (a) Model 1. (b) Model 2.

magnet magnetization orientation. After implementing the Halbach array configuration, the skewed magnet technique is applied to the Halbach PM array with two possible comparative configurations: namely the Halbach-array PM with only secondary PMs can be skewed (Model 1), as shown in Fig. 3(a) and the Halbach-array PM with primary PM and secondary PMs can be skewed (Model 2), as shown in Fig. 3(b). These designs are a favorable to create a flux-concentrated and flux-cancelling effect, maximizing interaction with the stator windings. This approach also facilitates partial cancellation of magnetic fields on one side. This flux-cancelling effect is another approach in minimizing losses and maximizing the productive magnetic flux where it is needed most, which improves a net magnetic field in the desired direction.

A comparison of these two configurations in-terms of their performance is presented in this paper. The design objectives are also based on the requirements in application to EVs, mainly to improve the torque capability, and torque density, reduce torque ripple and minimize magnet volume. The structural parameters of the benchmark structure, as well as optimal structure of the two skewed Halbach-array PM are shown in Table 1. The optimized configuration of these two models is achieved through the optimization procedure explained the next section.

III. DESIGN OPTIMIZATION

In order to achieve highest performance for the proposed dual skewed Halbach-array PM TORUS motor, both the Halbach-array and dual skewed PM configurations have been optimized. The optimization process as shown in Fig. 4. The following steps outline the further details

Step 1: Initialize the configuration of skewed Halbach-array PMs TORUS motors.

Step 2: Define objective functions and constraints.

Step 3: Select design variables and prioritize them through sensitivity analysis.

Step 4: Construct response surfaces for the prioritized design variables.

Step 5: Obtain the optimal structure of TORUS motors using response optimizer.

Step 6: Evaluate the performance of both TORUS motors and make a comparison to each other.

TABLE 1. Machine specifications.

Parameters (unit)	Benchmark	Model 1	Model 2
Axial length (mm)		60	
Stator outer radius (mm)		130	
Stator inner radius (mm)		65	
Air gap length (mm)		1	
Height of stator (mm)		38	
Height of stator yoke (mm)		12	
Width of stator yoke (mm)		13	
Length of stator yoke in radial direction (mm)		43	
Stator teeth outer width (mm)		29	
Stator teeth inner width (mm)		12	
Height of PM (mm)		5	
PM pole arc, α_{pa} (degree)		16.5	
PM pole pitch, α_{pp} (degree)		18	
α_{ur} (degree)	-	0.9	0.17
α_{lr} (degree)	-	0.53	1.18
α_{cl} (degree)	-	-0.42	-0.67
HB_{deg} (degree)	-	3.77	2.34

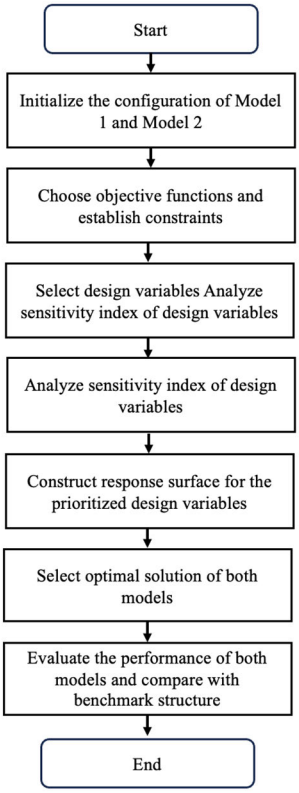

FIGURE 4. Flowchart indicating design optimization process.

A. OBJECTIVE FUNCTIONS AND CONSTRAINTS

In this study, as illustrated in Fig. 3 and 5, two variations of the skewed Halbach-array PM TORUS motors, namely Model 1 and Model 2 are considered. Both models are designed for application as EV traction motors and therefore the objective function is defined with a primary objective of maximizing average torque and secondary objective of minimizing torque ripple. The design constraints are defined such that:

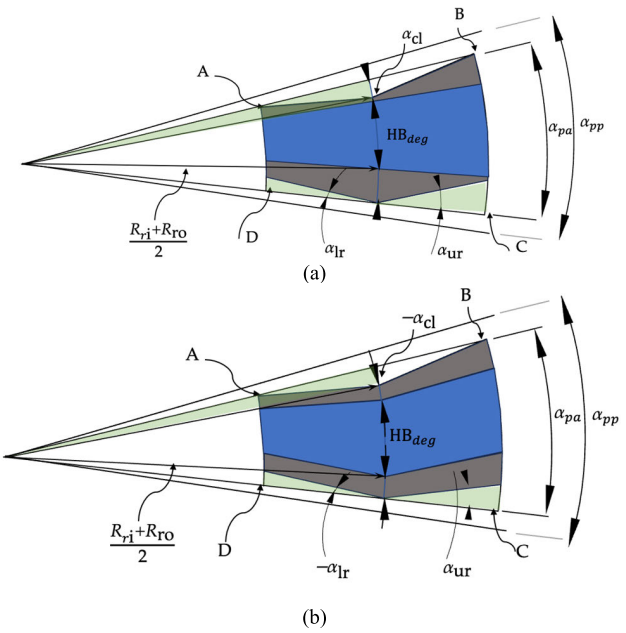

FIGURE 5. Design variables of the skewed Halbach-array PM TORUS motors. (a) Model 1. (b) Model 2.

1) Optimization is performed under the same current density and rated speed of 1,200 rpm when the current frequency is 200 Hz

2) Both machines utilize the same stator design as benchmark structure and has an inner and outer radius for the rotor fixed, as well as the length for the stack lamination is maintained to be the same as that of the benchmark machine

3) The proposed machine also employs the same core material and PM material as the benchmark structure, and

4) Volume of PM of both TORUS motors not greater than that of the conventional structure.

B. DESIGN VARIABLES AND SENSITIVITY ANALYSIS

The design variables for Model 1 and Model 2 of the proposed TORUS motors are depicted in Fig. 5. HB_{deg} is the arc angle of the center magnet, measured outward from the center of the pole arc at the midpoint between the inner rotor radius and the outer rotor radius. The skewing angles of the adjacent magnets are defined as following: α_{ur} represents the angle at the upper-right corner (point C), α_{lr} represents the angle at the bottom-right corner (point D), and α_{cl} signifies the angle at the left corners relative to point E. The reference point of these skewing angles is at the edge of the pole arc in which those angles are measured as the angle pointing toward the center of the pole. It should be noted that in the difference in configuration between Model 1 and Model 2 is primarily that the magnet of Model 2 will be skewed according to the values of α_{ur}, α_{br}, and α_{cl}, while the main middle magnet in Model 1 will remain non-skewed. It is important to note that the design parameters are varied according to their sensitivity-based constraints.

In the machine design and optimization, performing a sensitivity analysis of design variables is essential for

TABLE 2. Levels and related values of BBD of design variables.

Parameters (unit)	Model 1			Model 2		
	-1	0	1	-1	0	1
α_{ur} (degree)	0	2.5	5	0	2.5	5
α_{lr} (degree)	0	2.5	5	0	2.5	5
α_{cl} (degree)	-5	-2.5	0	-5	-2.5	0
HB_{deg} (degree)	0	2.5	5	0	2.5	5

TABLE 3. Sensitivity indices of design variables.

Parameters (unit)	Model 1			Model 2		
	$S_{T_{avg}}$	$S_{T_{rip}}$	Sensitivity level	$S_{T_{avg}}$	$S_{T_{rip}}$	Sensitivity level
α_{ur} (degree)	53.7%	4.7%	Higher	28.7%	15.8%	Higher
α_{lr} (degree)	23.3%	4.8%	High	9.6%	33.4%	High
α_{cl} (degree)	7.3%	33.9%	High	17.7%	8.6%	High
HB_{deg} (degree)	27.9%	97.9%	Higher	14.3%	41.6%	Higher

assessing the relative influence of these parameters on the design objectives. Therefore, prior to optimizing the design variables, the dependency of α_{ur}, α_{br}, α_{cl} and HB_{deg} have been analyzed through a sensitivity analysis. This process facilitates achieving optimal performance and also minimizes computational time. A comprehensive sensitivity index in percentage $S_i(\%)$ is used to quantify sensitivity:

$$S_i(\%) = \frac{\partial F(X)}{\partial x_i}|_{X=X_0} = \frac{F(X_0 + \Delta X_i) - F(X_0)}{\pm \Delta X_i} \times 100 \quad (1)$$

where $F(X)$ is objective function, X is the design variable, X_i is the value of the design variable, X_0 is the initial value of the design variable. Table 2 defines the variation range of design variables for sensitivity analysis, based on adjustable values relevant to the machine structure. To identify sensitivity indices of the design variables, randomly generated samples were obtained using the Box-Behnken Design (BBD), a strategic method for generating a well-distributed set of experimental points across the design space [24]. The related levels of the design variable range in BBD are represented by -1 (minimum value), 0 (central value), and 1 (maximum value). From Table 3, the comprehensive sensitivity indices of all design variables are detailed, focusing on the objectives of average torque, T_{avg}, and torque ripple, T_{rip}. Considering the EV-specific design objective, typically featuring a weight ratio between T_{avg} and T_{rip} of 0.8:0.2. From the results, it is noticeable that for both the models, parameters α_{ur} and HB_{deg} have higher sensitivity indices compared to that of α_{lr} and α_{cl}. As a result, these sensitivity findings will steer as constraints during subsequent optimization using RSM.

C. OPTIMIZATION OF DESIGN VARIABLES USING RSM

In this study, optimization based on RSM under sensitivity-based constraints is performed to identify the most suitable

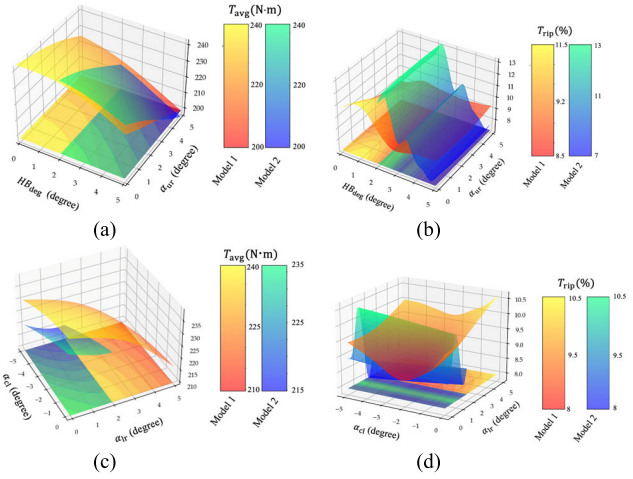

FIGURE 6. Surface plots of Model 1 and Model 2. α_{ur} and HB_{deg} versus (a) T_{avg} and (b) T_{rip}. α_{cl} and α_{lr} versus (c) T_{avg} and (d) T_{rip}.

TABLE 4. Optimizer settings based on BBD.

Output parameter (unit)	Objective	Min. value		Goal value	Max. value		Weight
		Model 1	Model 2		Model 1	Model 2	
Average torque (N·m)	Maximizing	220	230	250	-		0.8
Torque ripple (%)	Minimizing	-		10	13	13	0.2

values for all design variables. In this work, for the systematic creation of experiments in response surface analysis, randomly generated samples were obtained using the BBD. Equation (2) outlines the general form of a response surface model, where the corresponding response, Y, is given by:

$$\boldsymbol{Y = \beta_0 + \Sigma\left(\beta_i X_0\right) + \Sigma\left(\beta_{ii} X_i^2\right) + \Sigma\left(\beta_{ij} X_j\right) + \varepsilon} \quad (2)$$

where Y represent the response value, β_o is a constant term, β_i and β_{ii} are the first and second-order coefficients, respectively. The parameter β_{ij} denotes a second-order interaction term and ε represents the difference between the observed values of Y and that predicted by the model. It accounts for unobserved or random factors that influence the dependent variable Y, however but are not explicitly included in the response model.

Fig. 6 display the surface plots of the sensitivity-based design parameters versus the objective functions of Model 1 and Model 2, respectively. Each of the response surfaces of these machines are constructed from 25 actual experimental data points acquired through BBD. Results demonstrates that each design parameter exhibits a substantial influence on both T_{avg} and T_{rip}, affirming that optimizing these variables can greatly enhance the performance of both machines.

To determine the optimal values of the design variables, the optimizer selects them based on the objective functions, desired goal values, constraints, and weights, all tailored to the context of EV applications, as shown in Table 4. As illustrated in Fig. 7, the influence of the

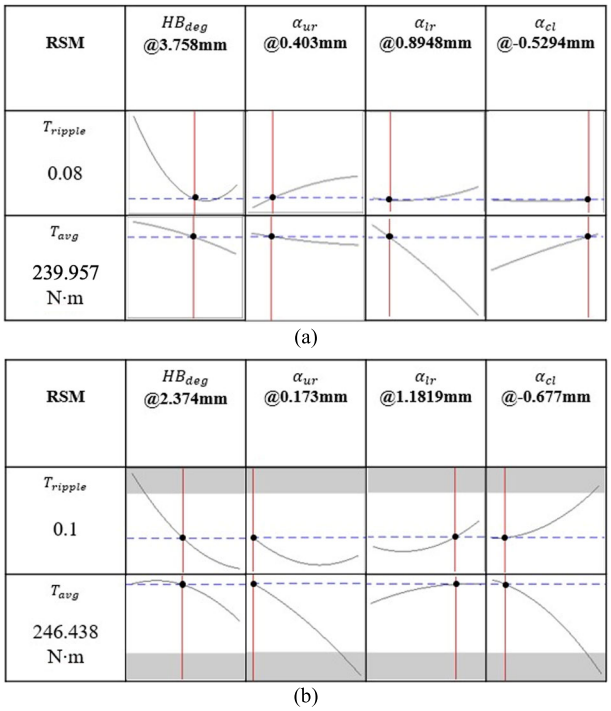

FIGURE 7. Influences on the design variables on motor performance at optimal solution. (a) Model 1. (b) Model 2.

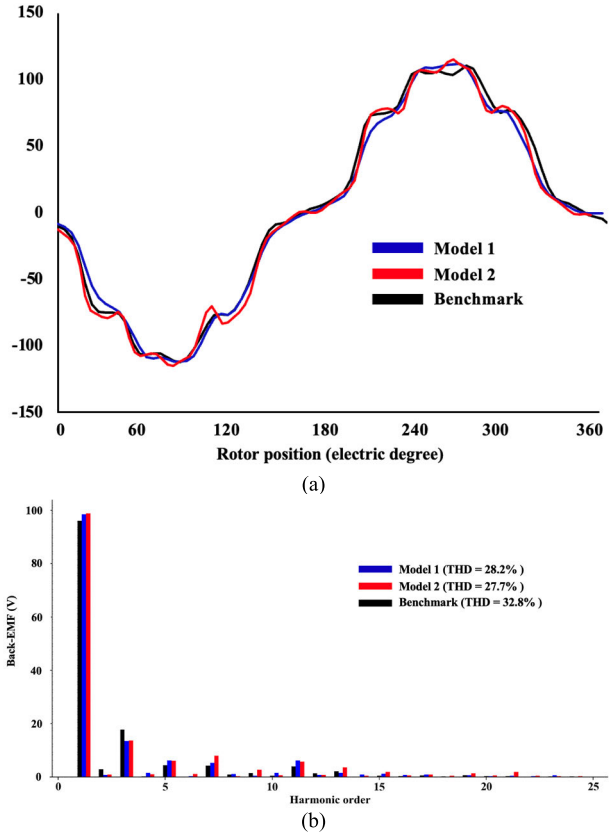

FIGURE 8. Open-circuit phase back-EMF. (a) Waveforms. (b) Harmonics.

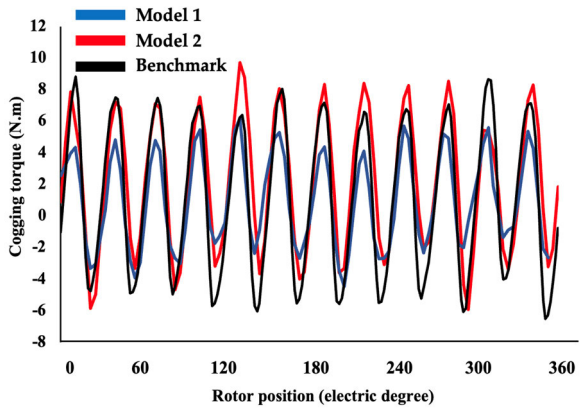

FIGURE 9. Comparison of cogging torque between two TORUS motors.

design variables on motor performance at optimal solution revealed that the optimal point of Model 1 occurs at $\alpha_{\rm ur} = 0.17$ degrees, $HB_{\rm deg} = 3.77$ degrees, $\alpha_{\rm lr} = 0.53$ degrees, and $\alpha_{\rm cl} = -0.42$ degrees, while that of Model 2 occurs at $\alpha_{\rm ur} = 0.17$ degree, $HB_{\rm deg} = 2.34$ degree, $\alpha_{\rm lr} = 1.18$ degree, and $\alpha_{\rm cl} = -0.67$ degree. With these optimal design values, Model 2 of proposed TORUS motor produces an average torque of 248.5 N·m and a torque ripple of 10.6%, while Model 1 produces an average torque of 242.6 N·m and a torque ripple of 11.22%. Comparison of torque capability between Model 1 and Model 2 clearly indicate that Halbach-array PM TORUS Model 2 achieves better performance. When compared to the benchmark machine, the Model 2 achieves an 8% improvement in average torque capability with a 7.8% reduction in torque ripple.

IV. PERFORMANCE EVALUATION

To validate the optimization process, the electromagnetic performance of the proposed skewed Halbach-array PM TORUS motors have been evaluated and compared with the benchmark motor using 3D finite element analysis. The comparison is conducted at a rated operating speed of 1200 rpm with an identical current density of the stator coils.

A. NO-LOAD PERFORMANCE

The no-load back-EMF profiles of the proposed TORUS motors are shown in Fig. 8 and are compared to the benchmark motor. Model 1 and Model 2 of the TORUS motors exhibit back-EMF values of 98.5 and 99.2 Vrms, respectively, representing 2.6% and 3.3% improvements over the benchmark. Analysis of the harmonic spectrum reveals that Model 2 has the lowest total harmonic distortion (THD) at 27.7%. Moving to Figure 9, the peak-to-peak cogging torque for Model 1 and Model 2 is measured at 10.3 and 14.5 N·m, respectively, indicating reduction of 35% and 9.3% compared to the benchmark. This reduction implies the superior performance of the TORUS motors during initial and low-speed operation, potentially minimizing torque ripple effects. In Fig. 10, a comparison of magnetic field

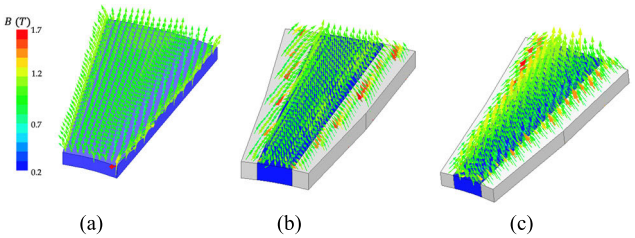

FIGURE 10. Comparison magnetic field distribution between two TORUS motors.

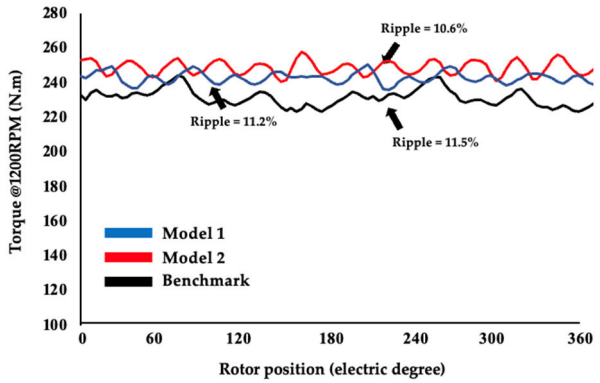

FIGURE 11. Comparison of torque waveforms between benchmark, Model 1, and Model 2 TORUS motors.

distribution is depicted. It illustrates that Model 2 exhibits a superior concentration of the magnetic field extending from the rotor PM to the armature winding area compared to Model 1 and the benchmark structure. This distribution directly affects the overall magnetic field passing through the armature winding area. The improved concentration in Model 1 and Model 2 is attributable to the Halbach-array PM arrangement which enhances magnetic field utilization, back-EMF, and electromagnetic torque. Moreover, the utilization of skewed PMs in both Model 1 and Model 2 provides a more uniform distribution of magnetic force between the stator and rotor, thereby contributing to reduced cogging torque. Overall, Model 2 demonstrates the highest no-load performance.

B. ON-LOAD PERFORMANCE

Figure 11 presents a comparative analysis of torque waveforms between the benchmark, Model 1, and Model 2. It highlights that Model 2 produces an average torque of 248.9 N.m, while Model 1 achieves 243.5 N.m. The average torque produced by Model 1 and Model 2 are 5.7% and 8.1% respectively, which is an improvement over the benchmark. Moreover, Model 2 exhibits a reduction in torque ripple from 11.5% of the benchmark to 10.6%, indicating enhanced operational smoothness as an EV motor. Conversely, Model 1 shows a slight reduction in torque ripple compared to the benchmark. The reduction in torque ripple in the proposed motors is attributed to the mitigation of flux harmonics through the integration of Halbach-array

TABLE 5. Comparison of electromagnetic performance at 1200 rpm.

Parameters (unit)	Benchmark	Model 1	Model 2
EMF (V_{rms})	96.0	98.5	99.2
Cogging torque ($N{\cdot}m_{p\text{-}p}$)	16	10.3	14.5
Rated current (A_{rms})		153.1	
Average torque (N·m)	230.2	242.86	248.52
Torque ripple (%)	11.5	11.22	10.6
PM volume (mm^3)	364,280	350,551	349,126
Torque density ($N{\cdot}m/mm^3$)	72,514	76,237	78,014
Torque/PM volume (N·m/L)	634	692	682
Efficiency (%)	93.5	93.9	94.2

and skewing PM techniques. These findings unequivocally confirm that the torque capability of Model 2 superior to that of the other motors compared in this study. For future designs, several techniques can be implemented to further reduce torque ripple. These include rotor segmentation, notching of stator or rotor teeth, adding magnetic flux barriers, and shifting the stator shoes. Table 5 provides a comprehensive comparison of the output characteristics of three motors. All machines operate at a rated speed of 1200 rpm while maintaining identical current densities of 17 A/mm. The comparison of torque capability shows that both proposed models exhibit higher torque density and torque/PM volume compared to the benchmark structure. The efficiency of Model 1 and Model 2 has been enhanced, reaching 93.9% and 94.2%, respectively. Notably, both Model 1 and Model 2 surpass the benchmark motor in every aspect while also incorporating a lower volume of PMs. This demonstrates that implementing the skewed PM and Halbach-array PM techniques in the TORUS motor not only enhances the machine's torque capability but also reduces its total cost. Particularly, the overall analysis clearly indicate that Model 2 exhibits the highest electromagnetic performance. Therefore, the findings demonstrate the superior performance of the skewed Halbach-array PM TORUS motor, making it an excellent choice for EV applications. For future projects, it is suggested to incorporate experimental validation.

V. CONCLUSION

The study compared and investigated the electromagnetic performance of TORUS motors utilizing combined skewed PM and Halbach-array PM techniques. Two configurations of skewed PM Halbach-array PM rotors were considered: Model 1, with only secondary PMs skewed, and Model 2, with both primary and secondary PMs skewed. These configurations were designed and compared using surface response optimization to meet performance requirements for EV applications. While both proposed TORUS motor models produce significantly improved EMF compared to the benchmark structure, Model 2 achieved the lowest THD. The cogging torque of both proposed models were shown to be lower. Improved average torque and lower

torque ripple were achieved for both proposed motors. Particularly, Model 2 was shown to produce the highest average torque of 248.9 Nm, which is 8.1% higher than the benchmark, while its ripple was shown to be 10.6% lower than the benchmark. The magnetic field distribution has been discussed and this paper provides the rationale behind this performance improvement, indicating that the skewed Halbach-array PM rotor configuration significantly enhances magnetic field utilization within the TORUS motor structure. The efficiency of both proposed TORUS motors has also been enhanced, reaching 93.9% and 94.2% for Model 1 and Model 2, respectively. Overall, both Model 1 and Model 2 outperform the benchmark motor in every aspect while also containing a lower volume of PMs. Particularly, Model 2 exhibits the highest electromagnetic performance. These findings confirm the effectiveness of implementing the combined techniques of skewed and Halbach-array PM arrangement for TORUS machines. The proposed motor is therefore considered as a promising choice for use for EV applications.

REFERENCES

[1] S. C. Oh and A. Emadi, "Test and simulation of axial flux-motor characteristics for hybrid electric vehicles," *IEEE Trans. Veh. Technol.*, vol. 53, no. 3, pp. 912–919, May 2004, doi: 10.1109/TVT.2004.827165.

[2] K. M. Rahman, N. R. Patel, T. G. Ward, J. M. Nagashima, F. Caricchi, and F. Crescimbini, "Application of direct-drive wheel motor for fuel cell electric and hybrid electric vehicle propulsion system," *IEEE Trans. Ind. Appl.*, vol. 42, no. 5, pp. 1185–1192, Sep. 2006, doi: 10.1109/TIA.2006.880886.

[3] M. Suphama, P. Seangwong, N. Fernando, J. Jongudomkarn, A. Siritaratiwat, and P. Khunkitti, "A novel asymmetric hybrid-layer del-shaped rotor interior permanent magnet motor for electric vehicles," *IEEE Access*, vol. 12, pp. 2793–2802, 2024, doi: 10.1109/ACCESS.2023.3347777.

[4] C. Nissayan, P. Seangwong, S. Chamchuen, N. Fernando, A. Siritaratiwat, and P. Khunkitti, "Modeling and optimal configuration design of flux-barrier for torque improvement of rotor flux switching permanent magnet machine," *Energies*, vol. 15, no. 22, p. 8429, Nov. 2022, doi: 10.3390/en15228429.

[5] F. Giulii Capponi, G. De Donato, and F. Caricchi, "Recent advances in axial-flux permanent-magnet machine technology," *IEEE Trans. Ind. Appl.*, vol. 48, no. 6, pp. 2190–2205, Nov. 2012, doi: 10.1109/TIA.2012.2226854.

[6] A. Cavagnino, M. Lazzari, F. Profumo, and A. Tenconi, "A comparison between the axial flux and the radial flux structures for PM synchronous motors," *IEEE Trans. Ind. Appl.*, vol. 38, no. 6, pp. 1517–1524, Nov. 2002, doi: 10.1109/TIA.2002.805572.

[7] V. Lounthavong, W. Sriwannarat, A. Siritaratiwat, and P. Khunkitti, "Optimal stator design of doubly salient permanent magnet generator for enhancing the electromagnetic performance," *Energies*, vol. 12, no. 16, p. 3201, Aug. 2019, doi: 10.3390/en12163201.

[8] W. Sriwannarat, P. Seangwong, V. Lounthavong, S. Khunkitti, A. Siritaratiwat, and P. Khunkitti, "An improvement of output power in doubly salient permanent magnet generator using pole configuration adjustment," *Energies*, vol. 13, no. 17, p. 4588, Sep. 2020, doi: 10.3390/en13174588.

[9] V. Simón-Sempere, A. Simón-Gómez, M. Burgos-Payán, and J.-R. Cerquides-Bueno, "Optimisation of magnet shape for cogging torque reduction in axial-flux permanent-magnet motors," *IEEE Trans. Energy Convers.*, vol. 36, no. 4, pp. 2825–2838, Dec. 2021, doi: 10.1109/TEC.2021.3068174.

[10] M. Aydin, S. Huang, and T. A. Lipo, "Torque quality and comparison of internal and external rotor axial flux surface-magnet disc machines," *IEEE Trans. Ind. Electron.*, vol. 53, no. 3, pp. 822–830, Jun. 2006, doi: 10.1109/TIE.2006.874268.

[11] M. Polat, A. Yildiz, and R. Akinci, "Performance analysis and reduction of torque ripple of axial flux permanent magnet synchronous motor manufactured for electric vehicles," *IEEE Trans. Magn.*, vol. 57, no. 7, pp. 1–9, Jul. 2021, doi: 10.1109/TMAG.2021.3078648.

[12] X. Sun, B. Su, S. Wang, Z. Yang, G. Lei, J. Zhu, and Y. Guo, "Performance analysis of suspension force and torque in an IBPMSM with V-shaped PMs for flywheel batteries," *IEEE Trans. Magn.*, vol. 54, no. 11, pp. 1–4, Nov. 2018, doi: 10.1109/TMAG.2018.2827103.

[13] P. Dück, P. Lesniewski, and B. Ponick, "Design and analysis of axial-flux permanent magnet synchronous machines as traction drives for electric vehicles," in *Proc. Int. Symp. Power Electron., Electr. Drives, Autom. Motion (SPEEDAM)*, Jun. 2016, pp. 376–381, doi: 10.1109/SPEEDAM.2016.7525883.

[14] R. Huang, Z. Song, H. Zhao, and C. Liu, "Overview of axial-flux machines and modeling methods," *IEEE Trans. Transport. Electrific.*, vol. 8, no. 2, pp. 2118–2132, Jun. 2022, doi: 10.1109/TTE.2022.3144594.

[15] F. Nishanth, J. Van Verdeghem, and E. L. Severson, "A review of axial flux permanent magnet machine technology," *IEEE Trans. Ind. Appl.*, vol. 59, no. 4, pp. 3920–3933, Jul. 2023, doi: 10.1109/TIA.2023.3258933.

[16] L. Jia, M. Lin, W. Le, N. Li, and Y. Kong, "Dual-skew magnet for cogging torque minimization of axial flux PMSM with segmented stator," *IEEE Trans. Magn.*, vol. 56, no. 2, pp. 1–6, Feb. 2020, doi: 10.1109/TMAG.2019.2951704.

[17] Z. Islam, F. Khan, B. Ullah, A. H. Milyani, and A. Ahmed Azhari, "Design and analysis of three phase axial flux permanent magnet machine with different PM shapes for electric vehicles," *Energies*, vol. 15, no. 20, p. 7533, Oct. 2022, doi: 10.3390/en15207533.

[18] M. Yousuf, F. Khan, J. Ikram, R. Badar, S. S. H. Bukhari, and J.-S. Ro, "Reduction of torque ripples in multi-stack slotless axial flux machine by using right angled trapezoidal permanent magnet," *IEEE Access*, vol. 9, pp. 22760–22773, 2021, doi: 10.1109/ACCESS.2021.3056589.

[19] I. P. Wiltuschnig, P. R. Eckert, D. G. Dorrell, and A. F. Flores Filho, "A study of the influence of quasi-Halbach arrays on a torus machine," *IEEE Trans. Magn.*, vol. 52, no. 7, pp. 1–4, Jul. 2016, doi: 10.1109/TMAG.2016.2514980.

[20] Z. Zhang, C. Wang, and W. Geng, "Design and optimization of Halbach-array PM rotor for high-speed axial-flux permanent magnet machine with ironless stator," *IEEE Trans. Ind. Electron.*, vol. 67, no. 9, pp. 7269–7279, Sep. 2020, doi: 10.1109/TIE.2019.2944033.

[21] R. Huang, C. Liu, Z. Song, and H. Zhao, "Design and analysis of a novel axial-radial flux permanent magnet machine with Halbach-array permanent magnets," *Energies*, vol. 14, no. 12, p. 3639, Jun. 2021, doi: 10.3390/en14123639.

[22] C. Huang, B. Kou, X. Zhao, X. Niu, and L. Zhang, "Multi-objective optimization design of a stator coreless multidisc axial flux permanent magnet motor," *Energies*, vol. 15, no. 13, p. 4810, Jun. 2022, doi: 10.3390/en15134810.

[23] Y. Wang, J. Lu, C. Liu, G. Lei, Y. Guo, and J. Zhu, "Development of a high-performance axial flux PM machine with SMC cores for electric vehicle application," *IEEE Trans. Magn.*, vol. 55, no. 7, pp. 1–4, Jul. 2019, doi: 10.1109/TMAG.2019.2914493.

[24] S.-H. Lee, Y.-J. Kim, K.-S. Lee, and S.-J. Kim, "Multiobjective optimization design of small-scale wind power generator with outer rotor based on Box–Behnken design," *IEEE Trans. Appl. Supercond.*, vol. 26, no. 4, pp. 1–5, Jun. 2016, doi: 10.1109/TASC.2016.2524620.

PHUSON SRIKHUMPHUN received the B.S. degree in electrical engineering from Khon Kaen University, Khon Kaen, Thailand, in 2021. He is currently pursuing the master's degree with the Department of Electrical Engineering, Faculty of Engineering. His research interests include electrical machine, permanent magnet machine, electrical vehicles, electrical motors, electrical generators, and renewable energy.

PATTASAD SEANGWONG received the B.S., M.S., and Ph.D. degrees in electrical engineering from Khon Kaen University, Khon Kaen, Thailand, in 2018, 2020, and 2023, respectively. His research interests include electrical machines, permanent magnet machines, electric vehicles, electrical motors, electrical generators, and renewable energy.

JONGGRIST JONGUDOMKARN received the B.Eng. and Dipl.-Ing. degrees in electrical engineering and information technology from the Technical University of Munich, Germany, in 2012 and 2013, respectively, and the Ph.D. degree from Osaka University, in 2020. He is currently an Assistant Professor with the Department of Electrical Engineering, Faculty of Engineering, Khon Kaen University, Thailand. His research interests include distributed generators, power quality, electric machine drives, and power conversion.

APIRAT SIRITARATIWAT received the B.Eng. degree in electrical engineering from Khon Kaen University, Thailand, in 1992, and the Ph.D. degree from The University of Manchester, U.K., in 1999. Subsequently, he gained industry experience and worked for a few years. In 1994, he joined the Department of Electrical Engineering, Khon Kaen University. He is currently with the KKU-Seagate Cooperation Research Laboratory, Department of Electrical Engineering, Faculty of Engineering, Khon Kaen University. He has been an Active Researcher in the fields of electrostatic discharge/electrical overstress (ESD/EOS) and electromagnetic interference (EMI) and has an impressive record of over 100 publications in these areas. Moreover, he is recognized as one of the pioneering researchers in the field of magnetism in Thailand. His significant contributions to this area include extensive work with hard disk drive (HDD) industries.

NUWANTHA FERNANDO received the B.Sc. degree in electrical engineering from the University of Moratuwa, Sri Lanka, in 2008, and the Ph.D. degree from The University of Manchester, U.K., in 2012. He was a Researcher with the University of Nottingham and the University of Oxford. He is currently a Lecturer with the Royal Melbourne Institute of Technology (RMIT), Melbourne. His research interests include electric machines and drives, with a specific emphasis on applications in electric transportation. He contributes as an Editor of IEEE TRANSACTIONS ON ENERGY CONVERSION.

SAKDA SOMKUN (Senior Member, IEEE) received the B.Sc.Tech.Ed. and M.Eng. degrees in electrical engineering from the King Mongkut's University of Technology North Bangkok, Bangkok, Thailand, in 2001 and 2003, respectively, and the Ph.D. degree in electrical and electronic engineering from the Wolfson Centre for Magnetics, Cardiff University, U.K., in 2010. He is currently an Associate Professor with the School of Renewable Energy and Smart Grid Technology, Naresuan University, Phitsanulok, Thailand. His current research interests include power electronics and electric drives.

PIRAT KHUNKITTI (Senior Member, IEEE) received the B.Eng. (Hons.) and Ph.D. degrees in electrical engineering from Khon Kaen University, Thailand, in 2012 and 2016, respectively. He is currently an Associate Professor with the Department of Electrical Engineering, Faculty of Engineering, Khon Kaen University. His research interests include electrical machines, permanent magnet machines, electric vehicles, electrical motors, electrical generators, and renewable energy. He was a recipient of numerous scholarships from Thailand Research Fund and the National Research Council of Thailand. He serves as an Editor for *Asia-Pacific Journal of Science and Technology*. He holds the role of an Assistant Editor of *Engineering and Applied Science Research*.